Characterization and in situ monitoring of large scale heap leach fluid dynamics

Jason Keller, GeoSystems Analysis, Inc., USA

Michael Milczarek, GeoSystems Analysis, Inc., USA

Tzung-mow Yao, GeoSystems Analysis, Inc., USA

Abstract

The efficiency of solution and air flow dynamics significantly affects metal recovery in heap leach operations. Quantifying these processes however presents extreme challenges. Laboratory and column scale measurements of physical and hydraulic properties of ore provide valuable information in aiding heap leach design and leaching operations; however, these measurements may not always be directly transferable to leach pad scale conditions. Consequently, the ability to operationally monitor cribs and heaps can be useful to quantify the effect of varying crush conditions, ore types, irrigation rates and, in the case of metal sulfide ores, aeration schemes on solution and aeration efficiency.

Depending on the desired monitoring parameters, monitoring systems can be designed to assess phreatic level surface, in situ solution content, oxygen content and temperature, and air injection pressures and air velocities. Sensors can be installed during heap construction or via coreholes or drive points to depths limited only by the achievable maximum depth of the chosen drilling method. Sensor installation can also be coordinated with a heap pad characterization program to determine in situ ore and permeability related properties at depth. Finally, field tracer tests can be used to determine solution transport properties and assess irrigation efficiency, the influence of macropores and preferential flow and solution retention times.

The selection and application of appropriate monitoring methods depends on the type of leaching operation (i.e. precious metal [cyanide] leach versus base metal [acid] leach), the leach pad size and duration of leaching. Cyanide leach solutions are less corrosive and heap temperatures typically approximate ambient conditions, which allows for more flexibility in sensor selection. In addition, air injection and oxygen concentration monitoring are not typically important, so monitoring instrumentation can focus on phreatic level and solution content/distribution monitoring. Conversely, acid leach heap

operations can benefit greatly from in situ temperature and oxygen monitoring, but these technologies require robust sensors to ensure long-term viability in elevated temperature and corrosive environments.

As a case study, we present the methodology and monitoring results from a large-scale copper heap leach pilot project. The pilot heap was designed to collect solution from different sectors of the heap to evaluate the efficiency of solution movement. Instrumentation was installed after the placement of ore material using drilling methods at various locations and at different depth intervals to monitor temperature, gaseous oxygen, solution content and capillary pressure. Monitoring data was collected in real time and transmitted to a control room with telemetry. Data collected from the monitoring program were used to validate initial field scale characterization and laboratory and column test results, and support industrial scale heap leach pad design and operation.

Introduction

In situ monitoring of solution and air flow within an active heap leach facility can provide useful information about the efficiency of the leaching process and create significant opportunities to improve metal recoveries. For example, solution content monitoring can determine when and whether the ore has been adequately wetted, while oxygen content and temperature monitoring can determine the distribution of air and temperature within the ore profile and whether aeration is sufficient/efficient. Laboratory and column scale measurements of physical and hydraulic properties of ore can provide valuable information in aiding heap leach design and leaching operations; however, these measurements may not always be directly transferable to leach pad scale conditions. Consequently, the ability to operationally monitor cribs and heaps can be useful to quantify the effect of varying crush conditions, ore types, irrigation rates and, in the case of copper sulfide ores, aeration schemes on solution and aeration efficiency. Moreover, in situ temperature, solution content, capillary pressure, solution chemistry, oxygen content, and air pressure and velocity measurements can be used to validate laboratory and field characterization tests and allow for real time adjustment of heap leach operations to increase leaching efficiencies.

In this paper, we provide an example of a 500,000 ton copper sulfide leach pad that was instrumented and monitored to investigate large-scale heap leach fluid dynamics under varying irrigation and aeration schemes, and describe a conceptual model of hydraulic flow in the heap derived from the monitoring data. The 18 m high heap had an approximately 90 m × 90 m leaching area. Prior to stacking, aeration lines were placed within an underlying gravel drainage layer to provide oxygen to the leach ore for enhancing bio-assisted leaching. Two air-line grids were established that allowed for the air source to originate from the east or from the west of the pad. Data collected from the 1.3 year monitoring program were used to validate initial field scale characterization and laboratory and column test results, and support industrial scale heap leach pad design and operation.

Methods

Instrumentation

The heap leach monitoring system consisted of:

- Nine 30 m by 30 m solution collection modules constructed beneath the gravel drainage layer.
- Nine boreholes (one per module) instrumented with temperature, oxygen/air piezometers, raffinate content, and capillary pressure sensors at 3 m intervals and at 0.5 m below ground surface (bgs).
- A phreatic surface sensor was installed 0.5 m above the gravel drainage layer, and suction lysimeters (for solution sampling) were installed at approximately 6 and 12 m bgs.
- 16 boreholes instrumented with temperature and oxygen/air piezometer sensors were installed at 3 m intervals.
- Raffinate content and capillary pressure sensors were installed at approximately 5, 11, and 16 m bgs.

A plan view of the heap as well as the location of instrument boreholes and solution collection modules relative to the leaching core are provided in Figure 1. The instrument boreholes were spatially located to provide data radiating from the center of the leaching core; 21 instrument boreholes were located within the leaching core and four instrument boreholes were located outside of the core to assess lateral migration of solution and air.

Instruments were installed in boreholes drilled with a 15 cm inside diameter hollow stem auger. All downhole instruments were attached to the outside of 2 inch diameter PVC pipe and the PVC was lowered inside the core barrel. The annulus between the monitoring instruments and the borehole wall was backfilled with:

- 10/20 mesh graded sand mixed 50:50 with ore surrounding the suction lysimeters;
- Leach ore surrounding the advanced tensiometers and raffinate content sensors;
- 3/8 inch gravel surrounding the air piezometers, oxygen sensors, and temperature sensors.

Backfill materials were added directly to the annulus of the borehole. A tag line was used to determine the correct backfill depth for each material. Bentonite chips were added above each backfill layer using a tremie pipe to seal between the instrument arrays and prevent surface and subsurface water, air, and/or heat from preferentially migrating down the borehole. The bentonite chips were hydrated after placement. All sensors were wired to data loggers for automated data collection; data loggers were connected to the central control room via telemetry.

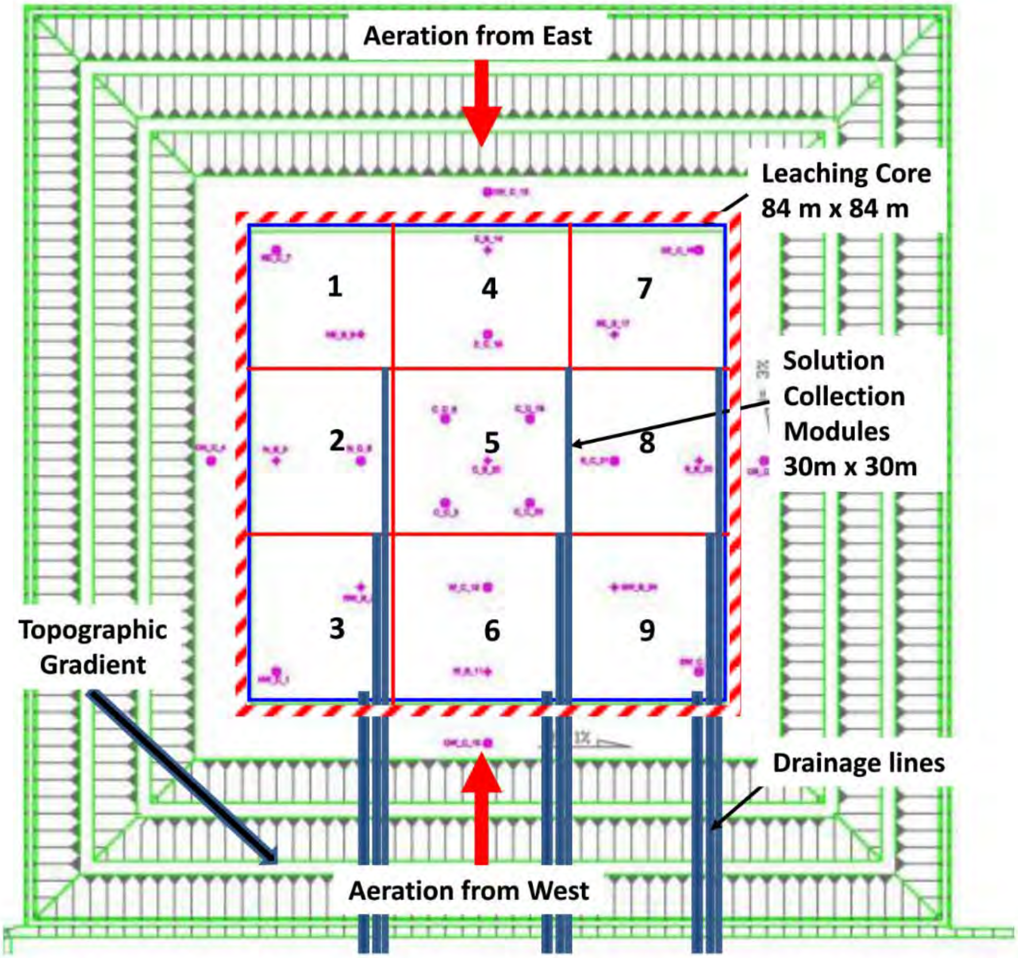

Figure 1: Plan view of heap instrument well locations and solution collection modules

Post test coring

Following completion of testing, sonic coring of 52 coreholes located within and around the leaching core of the heap was performed to collect samples for physical and hydraulic property testing. Geologic logging of the cores was also performed to estimate ore material texture and degree of oxidation (color). Particle size distribution (PSD) tests were performed on each 1.5 m interval.

Laboratory hydraulic analyses were performed on twelve composited cores selected to represent the range of particle size, core bulk density, predominant color characteristic (oxidized or un-oxidized ore), and module performance data. Consolidation permeability tests were conducted to determine the relationship of saturated and unsaturated hydraulic conductivity (Ksat and Kunsat) and air permeability to overburden pressures representing approximate sample depths within the heap. Details of the hydraulic test methods are described in a companion paper (Milczarek et al., 2013). The results of hydraulic property analyses were then correlated with particle size distribution data and sample depth to develop a predicted spatial distribution of heap hydraulic parameters across the heap.

Results

Estimated solution budget and drainage

An accounting of solution entering the heap and the estimated overall heap solution content is presented in Figure 2**Error! Reference source not found.**. The predicted volumetric solution content assumes an average initial water content of 0.12 cm^3/cm^3 (0.07 g/g) and that the difference between the irrigation and drainage equates to solution storage with correction for surface and heap evaporation (from elevated in situ temperatures and increased water holding capacity of air space). Predicted solution contents increased with the onset of double grid aeration, then decreased during the drainage phase of the study when irrigation was stopped (Figure 2). Predicted solution content increased again with the restart of irrigation and continued to steadily rise for the remainder of the project, to approximately 0.216 cm^3/cm^3 (21.6% volumetric), by the end of operation. The continued increase in storage represents solution going into storage within the leaching core and also represents any solution that moved laterally outside the core.

Figure 3 presents average normalized drainage, defined as drainage divided by irrigation, for module groupings along the north-south direction. Doubling the east aeration rate resulted in a significant drop in the normalized drainage from eastern modules 1, 4, 7 (0.76 to 0.18), a smaller decrease in the middle modules 2, 5, 8 (1.08 to 0.82) and a large increase in normalized drainage from western modules 3, 6, 9 (1.01 to 1.60). The effect of aeration direction is also observed during the alternating aeration period. Normalized drainage along the east side modules (1, 4, 7) decreased when the aeration source was from the east and increased when the aeration source was from the west. Similar behavior is observed with the west modules (3, 6, 9); normalized drainage from the west modules decreased during aeration from the west and increased when aeration was from the east. Note that normalized drainage from the middle modules (2, 5, 8) remained relatively stable during alternating aeration and that during the no aeration period, normalized drainage trends from the north-south module groups resembled the single east side aeration normalized drainage trends.

It is possible that damage to solution collection drainage pipes could account for some intercommunication of module solution or damage to aeration pipes could have resulted in irregular aeration distribution throughout the heap. Nonetheless, the correlation of aeration direction and rates to module drainage rates is strong, and is believed to be primarily caused by entrapped air within the leach ore and aeration back pressure within the drainage layer, as discussed further below.

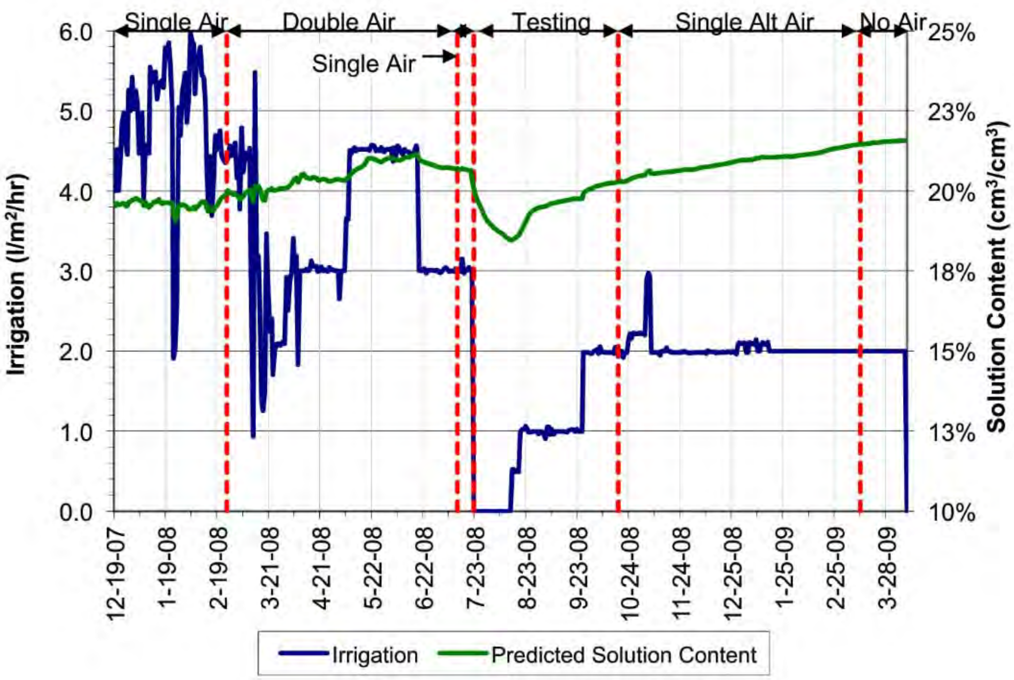

Figure 2: Irrigation rate over time and estimated solution budget

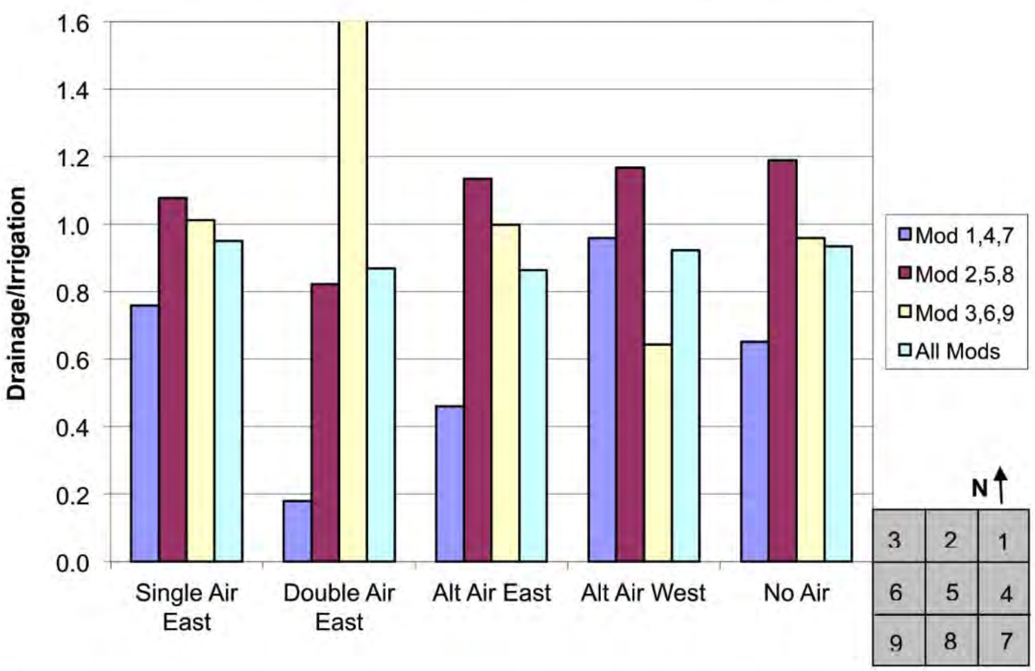

Figure 3: Average normalized drainage for module groups during different aeration schemes

Capillary pressure, phreatic surface, and temperature

Figure 4 provides soil water pressure potential (capillary pressure) contours interpolated from advanced tensiometer measured capillary pressures at 4 m bgs at various time periods representing single and double grid aeration from the east side. Capillary pressure data was also collected at 10 m and 15.5 m bgs but is not shown here due to space constraints. At all times capillary pressure was variable both laterally and with depth. Negative capillary pressures (< 0; orange and red) represent desired unsaturated leach conditions and very negative pressures (i.e. < –30 cm) indicate dry zones that may not be receiving sufficient solution. Conversely, positive capillary pressures (blue) may represent areas of entrapped air that reduce downward solution flow and result in perched solution conditions (pseudo-saturation). Figure 4 shows evidence of solution mounding at the 4 m bgs interval in Module 9 during both single and double aeration periods (mounding was also observed at 15.5 m bgs). Capillary pressure gradients can cause lateral solution movement following from high to low (more negative) capillary pressures. Of note, Module 9 showed below average drainage rates whereas adjacent, and upgradient, modules 5, 6 and 8 showed above average drainage rates, suggesting that solution was flowing laterally from Module 9 into these adjacent modules.

Capillary pressures generally increased as aeration went from single east to double east aeration (Figure 4). Capillary pressures subsequently decreased as aeration went to alternating aeration and then to no aeration. Specifically, the doubling of air injection rates resulted in increased capillary pressures which is most likely due to decreased leach ore hydraulic conductivity as air and solution competed for flow paths. As aeration decreased or was alternated from east-west, competition of air flow with solution flow was reduced and capillary pressures also decreased.

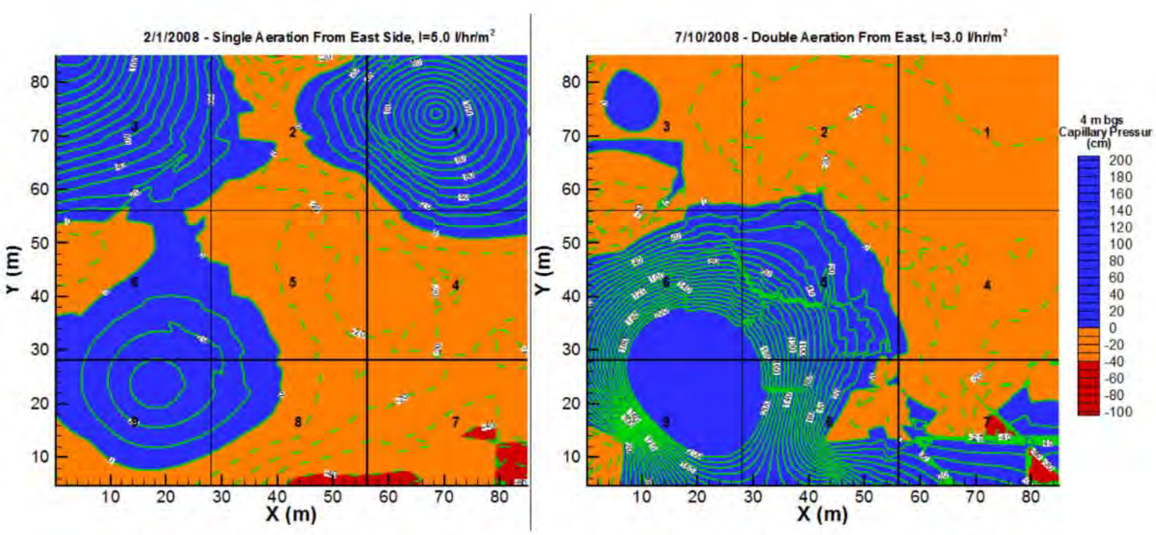

Figure 4: Capillary pressure contours at 4 m bgs at different time periods

Phreatic level monitoring 1.5 m above the drainage system liner (0.5 m into the leach ore), indicated the phreatic surface gradient corresponded to changes in aeration regimes (date not shown). Phreatic level changes also corresponded to changes in drainage rates; in general, as phreatic levels decreased, drainage rates increased and vice versa. The most probable mechanism for increased phreatic levels (and decreased drainage) is aeration back pressure within the underlying drainage layer and/or air entrapment in the leach ore above the drainage layer. This effectively reduces the leach ore permeability and solution pressure in the overlying leach ore must increase to allow the solution to drain. When aeration rates/pressures are reduced, entrapped air and back pressure dissipates and more pore space is available for solution movement. This results in increased leach ore permeability, which also increases the drainage rate and decreases the phreatic level.

Temperatures increased during the early period of heap operation and generally stabilized as double aeration from the east began (Figure 5). At the onset of increased irrigation (4.5 l/m^2/hr) on 5/7/2008 temperatures began to decrease and continued to decrease until irrigation was stopped on 7/23/2008. At this time temperatures began to increase and then generally stabilized during the alternating aeration scheme. Temperatures then decreased after aeration was stopped. Within the core of the heap, temperatures were within the optimum temperature range for bioleaching (30°C to 60°C) for the majority of operation. The increase in heap temperatures with the cessation of irrigation also coincided with an increase in oxygen (data not shown).

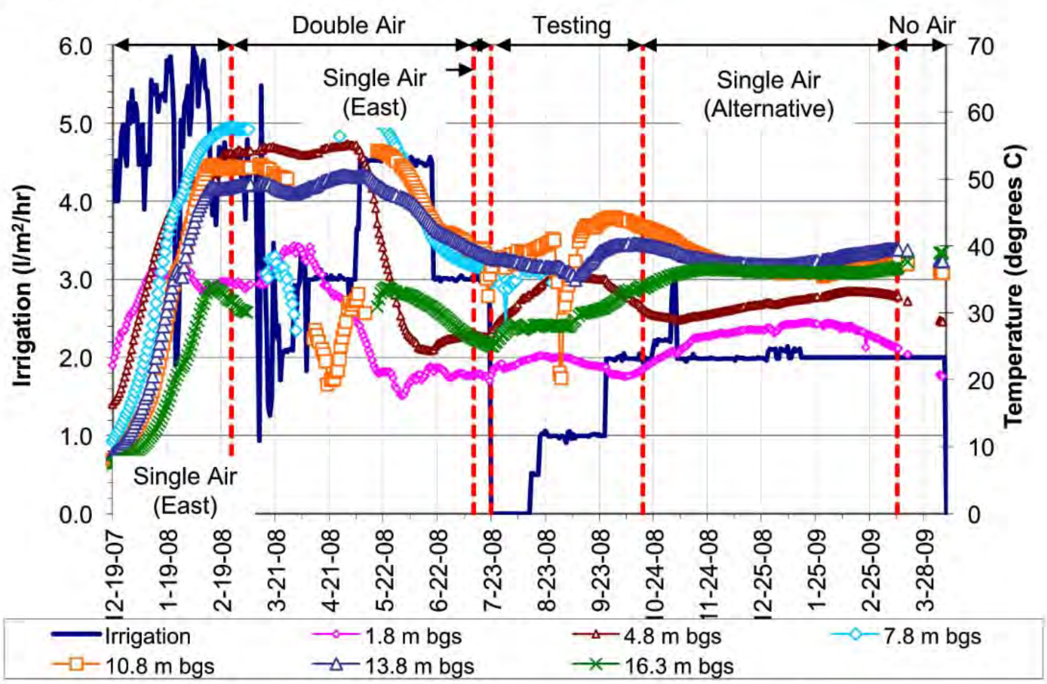

Figure 5: Leaching core temperature for Module 5

Post leach ore sampling and testing

Average PSD for all post-leach core samples and the average PSD for pre-leach ore material (after crushing and prior to agglomeration) indicated that leaching and decrepitation of the ore significantly increased the amount of material passing all mesh sizes, with material passing the #100 mesh increasing on average from 11.4 to 21.1% for pre-leach ore to post-leach ore (Figure 6). The post-leach ore was also more "well-graded", whereby the distribution of particles is more evenly distributed between sieve sizes. Well-graded ore material is easier to compact (higher bulk density), which reduces the leach ore permeability under in situ heap pressures.

The average percentage passing the #100 mesh versus the module percolation as a percentage of total heap percolation showed a trend of decreasing percolation with increasing percentage passing the #100 mesh (Figure 7). Excluding Module 9, which behaved as an outlier, a reasonable relationship between percentage passing the #100 mesh and percolation is obtained ($R^2 = 0.66$). As discussed above, Module 9 experienced solution mounding at the 4 m bgs and 15.5 m bgs depths; in addition, the 10 m bgs intermediate depth showed more negative pressures (much drier). There was an observed increase in fines at 3.5 m and 15.5 bgs in Module 9 which could be due to increased solution contact and ore decrepitation at those depths, whereas the intermediate depths showed much less decrepitation, most likely due to lateral movement of solution away from Module 9 into the adjacent modules.

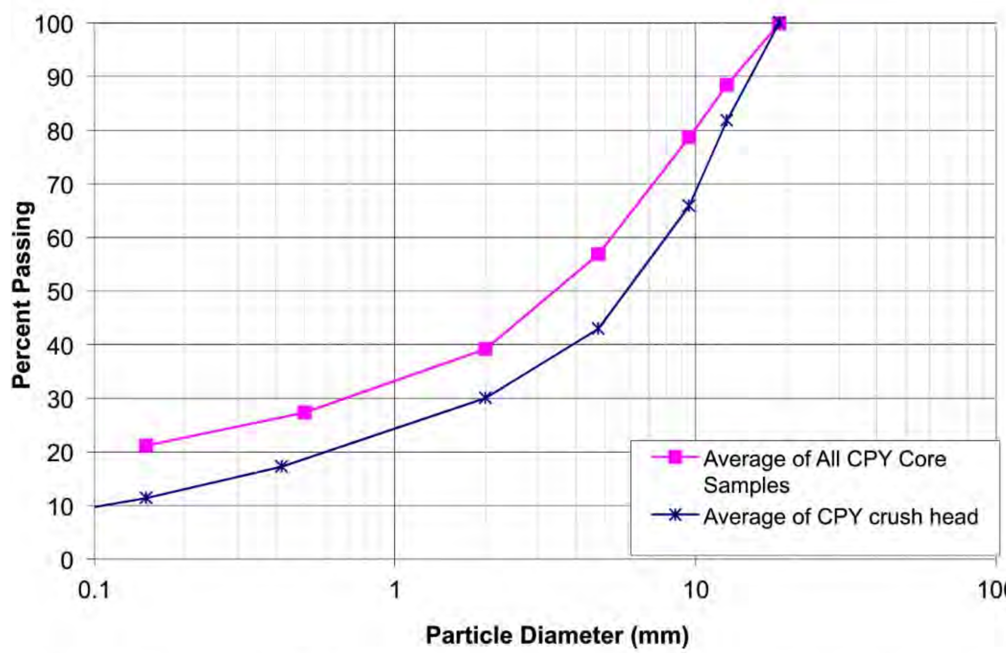

Figure 6: Average particle size distribution for all post-leach samples and crush head samples

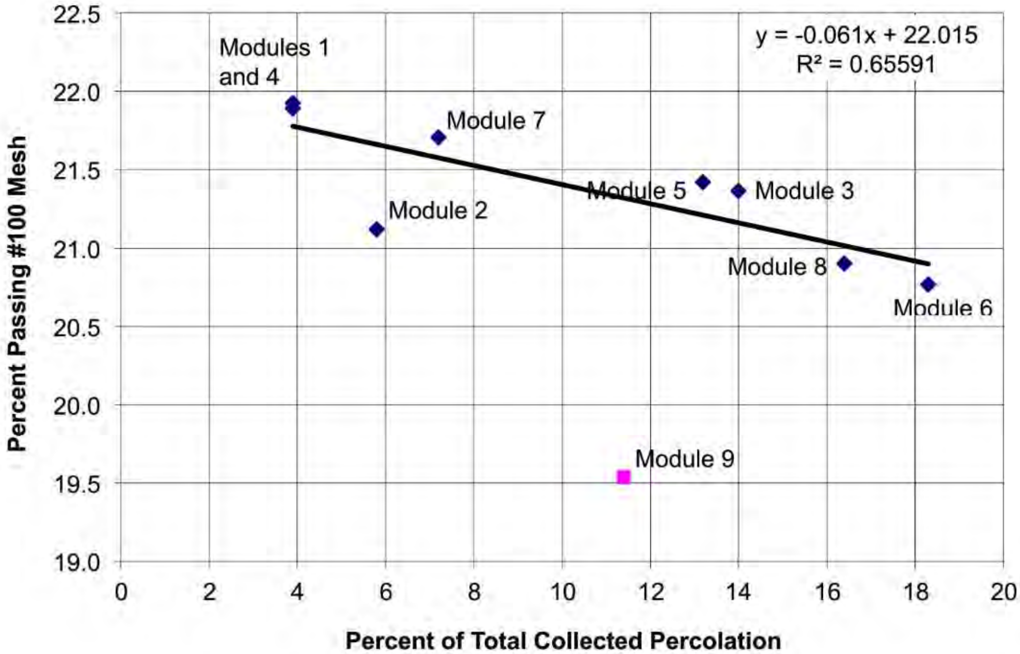

Figure 7: Average percentage passing the #100 mesh versus module percolation as a percentage of total heap percolation

Corehole logging indicated variable ore oxidation with the presence of jarosite (yellow ore) precipitates indicating oxidizing conditions and absence of precipitates (grey ore) indicating reducing conditions. The average percentage of total core that was yellow (oxidized ore) and percentage that was gray (reduced ore) is presented in Figure 8. Other precipitates (i.e. goethite) observed were generally less than a few percent within each module and are not presented. The average percentage of oxidized ore exceeded the average percentage of reduced ore in all modules, except for Module 9 and in coreholes located outside the perimeter of the modules (Figure 8). The greatest oxidation levels were observed in the eastern and western modules (except for Module 9) and also Module 5. Modules, 2, 8 and 9 showed the least oxidation. Higher oxidation in the eastern and western modules may be due to the proximity of these modules to the aeration source, whereas Module 9 most likely received less solution (and acid reagent) due to mounding and lateral flow from above 4 m bgs (see above). Lower oxidation levels in Modules 2 and 8 could be due to these modules being farther from the aeration source; however, Module 5 showed high oxidation levels which indicates there were potentially greater aeration losses from the north and south leaching core boundaries next to modules 2 and 8. Monitoring along these boundaries showed generally drier ore conditions. Finally, oxidation outside the leach core was also observed, indicating lateral movement of solution had leached ore outside of the irrigated core.

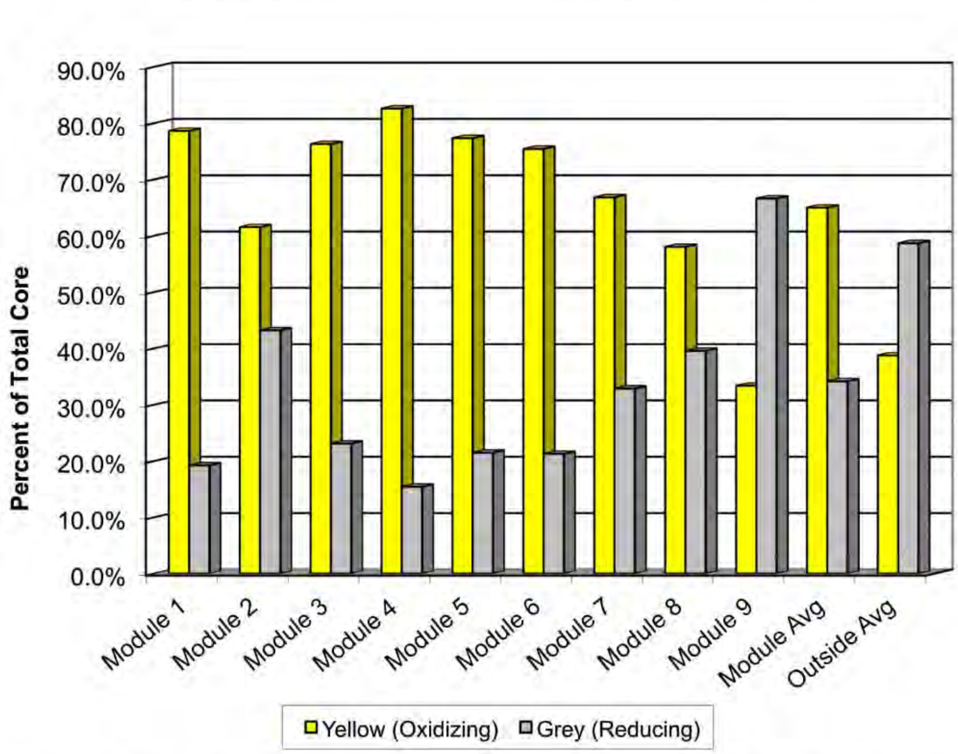

Figure 8: Module average percentage of yellow (oxidized) and grey (reduced) ore

Corehole samples selected for hydraulic property testing indicated that ore permeability decreased with increasing fines and bulk density values. Consolidation-permeability measured Ksat values showed strong correlation to a PSD indicator value which is described by:

- Fraction retained by the #4 mesh
- Fraction passing #100 mesh

The PSD indicator is a measure of the sorting of the leach ore with larger values representing poorly-graded material with a large fraction of gravel sized particles and smaller values representing well-graded material with higher percentage of fines. Multi-variate analysis of the average corehole measured PSD indicator and the estimated bulk density at each sample depth interval within individual modules (44 to 55 samples/module) resulted in a predicted Ksat (from the consolidation permeability data) of:

$$Log(Ksat) = 0.066xy + 0.011x^2 - 0.529x - 11.748 + 9.894y - 2.065y^2 \qquad R^2=0.76$$

Where x is depth in meters and y is the PSD indicator.

As was observed with the measured data, the predicted Ksat typically decreased with depth. Areas of increasing Ksat are predicted over module profiles due to increases in the PSD indicator or bulk density. Modules 1, 4 and 7 showed a lower predicted Ksat than other modules (due to the greatest amount of fines/decrepitation), which agreed with the observed data. However, the predicted Module 9 Ksat values did not agree with the poor percolation observed from this module. As discussed above, Module 9 appeared to have suffered from air entrapment and reduced permeability.

Conclusions

The in situ monitoring system allowed real-time monitoring of solution content, temperature, gaseous oxygen content and capillary pressure at various depths and locations in the heap. This allowed better understanding of the movement of solution and air in the heap leach facility and ultimately the efficiency of the leaching process. The initial air permeability of the heap was sufficient to develop high temperatures; however, in situ gaseous oxygen contents were observed to be variable and declined rapidly with a subsequent decline in in situ temperatures. Loss of aeration efficiency in the leaching core may have occurred due to reduced leach ore air permeability, which caused air to move laterally outside the core where ore conditions were drier and air permeability greater.

Individual module drainage rates were highly variable and decreased in proximity to the side where air was injected into the heap. Based on the drainage rate and phreatic level data, it is believed that aeration back pressure within the drainage layer caused solution mounding within the leach ore above the drainage rock. During aeration from the east, elevated phreatic levels at the leach ore/drainage layer interface caused lateral solution flow to down-gradient modules and reduced drainage from the eastern modules. This occurred most significantly during double grid east aeration and to a lesser extent during single grid east aeration. Phreatic level changes at the drainage layer were not large enough to result in solution moving from west to east. However, the movement of aeration to the west from the east reduced aeration back pressure in the eastern modules and increased drainage from the eastern modules and decreased drainage from the western modules. There was the potential for intercommunication of module solution resulting from damaged drainage collection piping or irregular aeration line distribution; however, the strong correlation of module drainage rates and the heap phreatic levels indicate that aeration back pressure within the drainage layer predominantly controlled solution flow behavior.

In addition, entrapped air at various locations higher in the leach ore may have resulted in increased capillary pressure and reduced hydraulic conductivity, which resulted in solution movement, as evidenced by low drainage rates from Module 9 and elevated drainage rates in adjacent modules. Module 9 also showed poor leach recovery below 4 m bgs where the high capillary pressure conditions were observed.

Solution was also observed to move outside of the leach core as evidenced by the capillary pressure data, high oxygen levels and presence of oxidized leach ore in the outside coreholes.

In situ monitoring indicated a solution and air flow system that is highly dynamic, multidimensional, and significantly influenced by the aeration system. Data collected during the in situ monitoring system allowed for a more complete understanding of the leach recovery dynamics.

Acknowledgements

This work would not have been possible without the support and collaboration over many years of BHP Billiton, Barrick Gold, Freeport McMoRan Copper and Gold, and Newmont Gold, under which our methods have been developed and tested.

References

Milczarek, M., Banerjee, M., Yao, T-m and Keller, J. (2013) Ore permeability methods of evaluation and applications to heap leach optimization. In *Proceedings of the Heap Leach International Conference 2013*, Vancouver, British Columbia, Canada.